

Phonon-assisted tunneling through a double quantum dot system

M. Bagheri Tagani, H. Rahimpour Soleimani,

Department of physics, University of Guilan, P.O.Box 41335-1914, Rasht, Iran

July 12, 2018

Abstract

Electron transport through a double quantum dot system is studied with taking into account electron-phonon interaction. The Keldysh nonequilibrium Green function formalism is used to compute the current and transmission coefficient of the system. The influence of the electron-phonon interaction, interdot tunneling, and temperature on the density of states and current is analyzed. Results show that although the electron-phonon interaction results in the appearance of side peaks in the conductance at low temperatures, they are disappeared in high temperatures.

1 Introduction

The study of transport through systems fabricated from two quantum dots has attracted a lot of attention during last decades because of their molecular-like behavior [1, 2, 3, 4, 5, 6, 7, 8]. Experimentally, quantum dots (QDs) can be in a serial or parallel configuration [1, 9]. Discreteness of energy levels, charging effects, and interdot tunneling in double quantum dot (DQD) systems result in novel and interesting phenomena such as: negative differential conductance (NDC) [5, 10], zero bias anomaly [11, 12], current rectification [9], Pauli spin blockade [13], ratchet effect [14], etc. Furthermore, a DQD system can be used to measure the lifetime of a singlet-triplet state [15]. DQD systems are also promising candidates for spintronic applications [16] and quantum computing [17, 18].

Coupling between the electronic and vibrational degrees of freedom can significantly affect the performance of the systems fabricated from QDs. The electron-phonon interaction (EPI) in nanostructures has been extensively studied both experimentally and theoretically [19, 20, 21, 22, 23, 24, 25, 26, 27, 28, 29]. Different models are used to investigate the influence of the EPI on the transport characteristics of the system such as: the rate equation approach [24, 30], the kinetic equation method [31], the Keldysh nonequilibrium Green function formalism [25, 26, 27], etc. Most work has been done on the single QD systems. However, the EPI in the DQD systems is an important and interesting subject needing more consideration.

In this work, we study the electron transport through a DQD system using the Keldysh nonequilibrium Green function formalism [32]. The issue has been recently analyzed by means of a rate equation approach [33]. It is assumed that the electrons of each dot interact with the vibrational degrees of freedom. The influence of the temperature, interdot tunneling, and EPI strength on the spectral function of each dot and transmission coefficient is examined. In the next section, the model used to describe the system is presented. Sec. 3 is devoted to the numerical results and in the end, some sentences are given as a summary.

2 Model and formalism

We consider two single level quantum dots attached to the metallic electrodes and assume that the electrons of each dot interact with a local vibrational mode. The Hamiltonian describing the whole system is given as ($\hbar = 1$)

$$H = \sum_{\alpha k} \varepsilon_{\alpha k} c_{\alpha k}^\dagger c_{\alpha k} + \sum_{i=L,R} \varepsilon_i d_i^\dagger d_i + t[d_L^\dagger d_R + H.C.] + \sum_i [\omega_i a_i^\dagger a_i + \lambda_i [a_i^\dagger + a_i] n_i] + \sum_{\alpha k i} [V_{\alpha k i} c_{\alpha k}^\dagger d_i + H.C.] \quad (1)$$

where $c_{\alpha k}^\dagger$ ($c_{\alpha k}$) creates (destroys) an electron with wave vector k , energy $\varepsilon_{\alpha k}$, in lead α whereas, d_i^\dagger (d_i) is the creation (annihilation) operator in the i th dot. The third term describes the interdot tunneling and t denotes the interdot tunneling strength. ω_i is the phonon energy in the dot i , while λ_i stands for EPI strength in the i th dot. We assume that each dot can have up to one electron. With respect to the fact that the energy levels of the QD are controlled using a gate voltage and, on the other hand, the on-site Coulomb repulsion is order of a few meV , the assumption is reasonable. Assuming weak lead-dot coupling, the EPI can be eliminated using nonperturbative canonical transformation [34], $\tilde{H} = e^S H e^{-S}$, where $S = \sum_i \lambda_i / \omega_i [a_i^\dagger - a_i] n_i$. Therefore, Eq.(1) becomes

$$\tilde{H} = \sum_{\alpha k} \varepsilon_{\alpha k} c_{\alpha k}^\dagger c_{\alpha k} + \sum_{i=L,R} \tilde{\varepsilon}_i d_i^\dagger d_i + t[X_L^\dagger X_R d_L^\dagger d_R + H.C.] + \sum_i \omega_i a_i^\dagger a_i + \sum_{\alpha k i} [V_{\alpha k i} X_i c_{\alpha k}^\dagger d_i + H.C.] \quad (2)$$

where $\tilde{\varepsilon}_i = \varepsilon_i - \lambda_i^2 / \omega_i$ is the renormalized energy level of the i th dot due to the polaronic shift and, $X_i = e^{-\frac{\lambda_i}{\omega_i} [a_i^\dagger - a_i]}$ is the phonon shift generator operator. Since the dot-lead coupling strength is weaker than the EPI strength, i.e., $V_{\alpha k i} \ll \lambda_i$, X_i is replaced with its expectation value, i.e., $X_i = \langle X_i \rangle = e^{-g_i (2N_{ph,i} + 1)}$, where $g_i = (\lambda_i / \omega_i)^2$, and $N_{ph,i}$ denotes the phonon population expressed as $N_{ph,i} = (\exp(\beta \omega_i) - 1)^{-1}$ with $\beta = 1/k_B T$. In the following, it is assumed that both QDs have the same shape and size so that the phonon

energy and EPI strength are independent of the QDs indexes and are shown by ω_0 , and λ , respectively.

In order to compute the current, the Keldysh nonequilibrium Green function formalism and wide band approximation are used so that the current can be expressed as [35]

$$I = \frac{e}{2h} \int d\omega \{Tr[(f_L(\omega)\Gamma^L - f_R(\omega)\Gamma^R)A(\omega)] + Tr[(\Gamma^L - \Gamma^R)(iG^<(\omega))]\} \quad (3)$$

where $f_\alpha(\omega)(1 + \exp((\omega - \mu_\alpha)\beta))^{-1}$ is the Fermi distribution function of the lead α , and μ_α denotes the chemical potential of the lead. $A(\omega)$ and $G^<(\omega)$ are the Fourier transformations of the spectral function and lesser Green function, respectively. The matrix Γ^α describes the tunneling coupling between the α th dot and the leads given as

$$\Gamma^L = \begin{pmatrix} \Gamma_0 & \sqrt{\alpha}\Gamma_0 \\ \sqrt{\alpha}\Gamma_0 & \alpha\Gamma_0 \end{pmatrix} \quad \Gamma^R = \begin{pmatrix} \alpha\beta\Gamma_0 & \beta\sqrt{\alpha}\Gamma_0 \\ \beta\sqrt{\alpha}\Gamma_0 & \beta\Gamma_0 \end{pmatrix} \quad (4)$$

where Γ_0 is a constant, α describes the difference in the coupling of the electrodes to different QDs, and β stands for asymmetry in the coupling of the QDs to the left and right leads. The spectral function is computed as

$$A(\omega) = i(G^>(\omega) - G^<(\omega)) = i(G^r(\omega) - G^a(\omega)) \quad (5)$$

where $G^{r(a)}(\omega)$ is the retarded (advanced) Green function of the whole system. To compute $G^{<(>)}(\omega)$ we follow the procedure introduced in Ref. [27]. Because the phonon shift generator operator is replaced with its expectation value, the Green functions can be separated to the electron and phonon parts as

$$G_{ij}^>(t) = -i \langle d_i(t)d_j^\dagger(0) \rangle = \tilde{G}_{ij}^>(t)e^{-\Phi(t)} \quad (6a)$$

$$G_{ij}^<(t) = i \langle d_j^\dagger(0)d_i(t) \rangle = \tilde{G}_{ij}^<(t)e^{-\Phi(-t)} \quad (6b)$$

where $i(j) = 1, 2$ stands for the matrix elements, $\tilde{G}^{<(>)}(t)$ is the dressed lesser (greater) Green function resulting from the electronic part of Eq.(2), and $e^{-\Phi(t)}$ comes from the phonon part, $\langle X(t)X^\dagger(0) \rangle$, given as [34]

$$e^{-\Phi(t)} = g[N_{ph}(1 - e^{i\omega_0 t}) + (N_{ph} + 1)(1 - e^{-i\omega_0 t})] \quad (7)$$

Using the identity $e^{-\Phi(t)} = \sum_n L_n e^{-in\omega_0 t}$, $G^{<(>)}(\omega)$ can be expressed as

$$G^>(\omega) = \sum_n L_n \tilde{G}^>(\omega - n\omega_0) \quad (8a)$$

$$G^<(\omega) = \sum_n L_n \tilde{G}^<(\omega + n\omega_0) \quad (8b)$$

where L_n is a function of temperature, T, EPI strength, and phonon population given as [27]

$$L_n = \frac{e^{-g}g^n}{n!} \quad \text{for } n \succeq 0 \quad \text{if } T = 0 \quad (9)$$

$$L_n = e^{-g(2N_{ph}+1)} e^{\frac{n\omega_0\beta}{2}} I_n(2g\sqrt{N_{ph}(N_{ph}+1)}) \quad \text{if } T \neq 0$$

where I_n is the n th Bessel function of complex argument. $\tilde{G}^<(\omega)$ can be computed using the Keldysh equation and Langreth analytical continuation as $\tilde{G}^<(\omega) = \tilde{G}^r(\omega)\tilde{\Sigma}^<(\omega)\tilde{G}^a(\omega)$, where $\tilde{\Sigma}^<(\omega) = i[\tilde{\Gamma}_L f_L(\omega) + \tilde{\Gamma}_R f_R(\omega)]$, and $\tilde{\Gamma}_\alpha = \Gamma_\alpha < X >^2$. Indeed, contribution to $\Sigma^<$ from electron-phonon interaction is disregarded due to weak electron-phonon interaction. In order to compute the dressed retarded Green function, the equation of motion technique is used. It is straightforward to show that the matrix elements of the Green function satisfy the following equation

$$[\omega - \tilde{\varepsilon}_i - \tilde{\Sigma}_{ii}]\tilde{G}_{ii}^r(\omega) = 1 + (t + \tilde{\Sigma}_{i\bar{i}})\tilde{G}_{i\bar{i}}^r(\omega) \quad (10a)$$

$$[\omega - \tilde{\varepsilon}_i - \tilde{\Sigma}_{ii}]\tilde{G}_{i\bar{i}}^r(\omega) = (t + \tilde{\Sigma}_{i\bar{i}})\tilde{G}_{\bar{i}\bar{i}}^r(\omega) \quad (10b)$$

where $\bar{i} = 2$ if $i = 1$, $\bar{i} = 1$ if $i = 2$, and $\tilde{\Sigma} = -i/2[\tilde{\Gamma}_L + \tilde{\Gamma}_R]$. Indeed, the real part of the self energy causing slightly shift in the QD energy levels is ignored (wide band approximation). With respect to Eq.(10), the retarded Green function is obtained as

$$\tilde{G}^r(\omega) = \frac{1}{P(\omega)} \begin{pmatrix} \omega - \tilde{\varepsilon}_2 - \tilde{\Sigma}_{22} & t + \tilde{\Sigma}_{12} \\ t + \tilde{\Sigma}_{21} & \omega - \tilde{\varepsilon}_1 - \tilde{\Sigma}_{11} \end{pmatrix} \quad (11)$$

where

$$P(\omega) = (\omega - \tilde{\varepsilon}_1 - \tilde{\Sigma}_{11})(\omega - \tilde{\varepsilon}_2 - \tilde{\Sigma}_{22}) - (t + \tilde{\Sigma}_{12})(t + \tilde{\Sigma}_{21}) \quad (12)$$

The Green function of the whole system can be written as [36]

$$\begin{aligned} G_{ij}^r(t) &= -i\Theta(t) \langle \{d_i(t), d_j^\dagger(0)\} \rangle = \tilde{G}_{ij}^r(t) \langle X(t)X^\dagger(0) \rangle \\ &\quad - \Theta(t)\tilde{G}_{ij}^<(t) [\langle X^\dagger(0)X(t) \rangle - \langle X(t)X^\dagger(0) \rangle] \end{aligned} \quad (13)$$

where after Fourier transformation, it becomes

$$G^r(\omega) = \sum_n L_n [\tilde{G}^r(\omega - n\omega_0) - \frac{1}{2}\tilde{G}^<(\omega + n\omega_0) + \frac{1}{2}\tilde{G}^<(\omega - n\omega_0)] \quad (14)$$

For simulation purposes, ω_0 is used as energy unit [37], and it is assumed that the energy levels of the QDs are degenerate so that the density of states of the QDs are identical shown by $A(\omega)$.

3 Results and discussions

Fig. 1 shows the density of states as a function of energy for different λ s and t s. In fig. 1a that $t = \Gamma_0$, there is a delta-like peak in the bonding state ($\tilde{\varepsilon}_i - t$) and a Lorentzian peak in the antibonding state ($\tilde{\varepsilon}_i + t$). For weak λ s, the below relation is obtained for $A(\omega)$ at the bonding and antibonding states

$$A(\tilde{\varepsilon}_i \pm t) = 4\tilde{\Gamma}_0 \frac{8t^2(1 \pm \sqrt{\alpha})^2 + \tilde{\Gamma}_0^2(1 + \alpha)(1 - \alpha)^2}{\tilde{\Gamma}_0^4(1 - \alpha)^4 + 16(1 \pm \sqrt{\alpha})^4 t^2 \tilde{\Gamma}_0^2} \quad (15)$$

For strong λ s, the bonding and antibonding states are farther from each other due to the red shift. Furthermore, satellite peaks are well observed in strong EPI coming from the phonon emission by electrons (at negative energies) and the phonon emission by holes (at positive energies). Note that the probability of the phonon absorption is zero in zero temperature because of $N_{ph} = 0$. As one expects, the spacing between the satellite peaks is equal to the phonon energy. The influence of the interdot tunneling strength on $A(\omega)$ is analyzed in fig. 1b. At $t/\Gamma_0 \ll 1$, the bonding and antibonding states are merged. With increase of t , these states are well separated. It is interesting to note that although the density of states are independent of the chemical potential of the leads in elastic transport, it is dependent on the position of the chemical potential of the leads in the presence of the EPI according to Eq.(5). However, the dependence does not affect significantly on $A(\omega)$.

The influence of the temperature on $A(\omega)$ is plotted in fig. 2. With increase of the temperature, the height of the peaks is increased whereas, their width is reduced. Such behavior was previously reported about a single level QD [27]. The dressing effect is increased by increase of T , so that $\bar{\Gamma}$ becomes smaller and, with respect to the fact that the width of the spectral function is related to the broadening, increase of the temperature results in the reduction of the width of the peaks. In addition, the probability of the phonon absorption is increased by increasing T and, as a result, the satellite peaks in $A(\omega)$ result from both the phonon emission and the phonon absorption. Unlike the elastic transport, the spectral function depends on the Fermi distribution of the leads in inelastic transport so that height of the peaks is increased by increase of the temperature owing to spreading the Fermi function by increase of T .

Transmission coefficient, $T(\omega) = Tr(G^a \Gamma^R G^r \Gamma^L)$, is shown in fig. 3 in zero temperature. There are two main peaks located in the bonding and antibonding states and a antiresonance-like behavior due to the destructive interference between different pathways through the system. The effect was before announced for a coupled QD system [38]. With increase of the EPI strength, the position of the bonding and antibonding states is shifted toward left. Furthermore, the secondary peaks are well observed resulting from the existence of the new channels for the electron transport because of the electron-phonon coupling. The probability of the electron transport through these channels is lesser than the probability of the electron transport through the main channels. The effect of the dot-lead coupling on $T(\omega)$ is studied in fig. 3b. Such analysis was before done without considering the EPI [38]. In serial configuration ($\alpha = 0$), the transmission coefficient exhibits two Lorentzian peaks centered at the bonding and antibonding states, respectively. In addition, the satellite peaks due to the phonon-assisted tunneling are clearly observed. With increase of α , the antiresonance-like behavior is also observed because of the destructive interference.

Fig. 4 shows the current-voltage characteristic of the system for different temperatures. In zero temperature, the current exhibits step-like behavior so that there is a step when the bonding or antibonding state is located inside the bias window. More steps are observed in the presence of the EPI because of

the phonon-assisted tunneling. The side peaks are well seen in the conductance spectrum. With increase of the temperature, the step-like behavior is vanished. Indeed, the electrons gain more energy to tunnel through the system owing to the thermal excitation. On the other hand, the effects coming from the EPI are not observed in the high temperature so that there is only one peak in the conductance.

4 Summary

The Keldysh nonequilibrium Green function formalism is used to study the electron transport through a double single level quantum dot system in the presence of the electron-phonon interaction. The behavior of the system is analyzed in both zero and nonzero temperatures using the nonperturbative canonical transformation. The current voltage characteristic exhibits the step-like behavior in low temperatures because of the EPI whereas, such behavior is disappeared at high temperatures. The influence of the temperature, EPI strength, and interdot tunneling strength on the transmission coefficient and density of states is also examined.

References

- [1] W. G. van der Wiel, S. De Franceschi, J. M. Elzerman, T. Fujisawa, S. Tarucha, L. P. Kouwenhoven, *Rev. Mod. Phys.* 75, 1 (2003).
- [2] R. Hanson, L. P. Kouwenhoven, J. R. Petta, S. Tarucha, L. M. K. Vandersypen, *Rev. Mod. Phys.* 79, 1217 (2007).
- [3] T. Hayashi, T. Fujisawa, H. D. Cheong, Y. H. Jeong, Y. Hirayama, *Phys. Rev. Lett.* 91, 226804 (2003).
- [4] G. Kießlich, E. Schöll, T. Brandes, F. Hohls, R. J. Haug, *Phys. Rev. Lett.* 99, 206602 (2007).
- [5] F. Chi, S-S. Li, *J. Appl. Phys.* 97, 123704 (2005).
- [6] F. H. L. Koppens, C. Buizert, I. T. Vink, K. C. Nowack, T. Meunier, L. P. Kouwenhoven, L. M. K. Vandersypen, *J. Appl. Phys.* 101, 081706 (2007).
- [7] F. Molitor, S. Droscher, J. Güttinger, A. Jacobsen, C. Stampfer, T. Ihn, K. Ensslin, *Appl. Phys. Lett.* 94, 222107 (2009).
- [8] W.H. Lim, H. Huebl, L.H. Willems van Beveren, R.G. Clark, A.S. Dzurak, *Appl. Phys. Lett.* 94, 173502 (2009).
- [9] K. Ono, D. G. Austing, Y. Tokura, S. Tarucha, *Science* 297, 1313 (2002).
- [10] I. Weymann, J'zef Barna's, *Phys. Rev. B* 73, 033409 (2006).

- [11] R. Aguado, D. C. Langreth, *Phys. Rev. Lett.* 85, 1946 (2000).
- [12] F. Chi, S-S. Li, *J. Appl. Phys.* 99, 043705 (2006).
- [13] A. C. Johnson, J. R. Petta, C. M. Marcus, M. P. Hanson, A. C. Gossard, *Phys. Rev. B* 72, 165308 (2005).
- [14] V. Moldoveanu, B. Tanatar, *Phys. Rev. B* 82, 205312 (2010).
- [15] J. R. Prance, Zhan Shi, C. B. Simmons, D. E. Savage, M. G. Lagally, L. R. Schreiber, L. M. K. Vandersypen, Mark Friesen, Robert Joynt, S. N. Coppersmith, M. A. Eriksson, arXiv:1110.6431v2 (2011).
- [16] *Semiconductor Spintronics and Quantum Computation*, edited by D. D. Awschalom, D. Loss, N. Samarth (Springer, Berlin, 2002).
- [17] D. Loss, E. V. Sukhorukov, *Phys. Rev. Lett.* 84, 1035 (2000).
- [18] R. Hanson, G. Burkard, *Phys. Rev. Lett.* 98, 050502 (2007).
- [19] H. Park, J. Park, A. K. L. Lim, E. H. Anderson, A. P. Alivisatos, P. L. McEuen, *Nature* 407, 57 (2004).
- [20] B.J. LeRoy, S.G. Lemay, J. Kong, C. Dekker, *Nature* 432, 371, (2004).
- [21] J. Yang, Y. Q. Gao, J. Wu, Z. M. Huang, X. J. Meng, M. R. Shen, J. L. Sun, J. H. Chu, *J. Appl. Phys.* 108, 114102 (2010).
- [22] Z. W. Wang, S. S. Li, *J. Appl. Phys.* 110, 043512 (2011).
- [23] B. Y. Choi, S. J. Kahng, S. Kim, H. Kim, H. W. Kim, Y. J. Song, J. Ihm, Y. Kuk, *Phys. Rev. Lett.* 96, 156106 (2006).
- [24] B. Dong, X.L. Lei, N. J. M. Horing, *Appl. Phys. Lett.* 90, 242101 (2007).
- [25] M. Galperin, M. A Ratner, A. Nitzan, *J. Phys.: Condens. Matter* 19, 103201 (2007).
- [26] U. Lundin, R. H. McKenzie, *Phys. Rev. B* 66, 075303 (2002).
- [27] Z. Z Chen, R. Lü, B. F. Zhu, *Phys. Rev. B* 71, 165324 (2005).
- [28] Y. S Liu, H. Chen, X. H. Fan, X. F. Yang, *Phys. Rev. B* 73, 115310 (2006).
- [29] A. Ueda, M. Eto, *New J. Phys.* 9, 119 (2007).
- [30] L. Siddiqui, A. W. Ghosh, S. Datta, *Phys. Rev. B* 76, 085433 (2007).
- [31] K. D. McCarthy, N. Prokofev, M. T. Tuominen, *Phys. Rev. B* 67, 245415 (2003).
- [32] H. Huag, A. P. Jauho, in *Quantum Kinetics in Transport and Optics of Semiconductors*, edited by Dr. -Ing. Helmut K. V. Lotsch (Springer-Verlag, Berlin Heidelberg, 1996).

- [33] M. B. Tagani, H. R. Soleimani, *Physica B* 406, 4056 (2011).
- [34] G. D. Mahan, *Many-Particle Physics*, 3rd ed. (Plenum Press, New York, 2000).
- [35] Y. Meir, N. S. Wingreen, *Phys. Rev. Lett.* 68, 2512 (1992).
- [36] W. Rudzin'sky, *J. Phys.: Condens. Matter* 20, 275214 (2008).
- [37] For generic values of ω see Refs. [19, 20]
- [38] M. L. Ladrón de Guevara, F. Claro, P. A. Orellana, *Phys. Rev. B* 67, 195335 (2003).

Figure captions

Figure 1: Density of states as a function of energy in zero temperature. Parameters are $\varepsilon_i = 0$, $\mu_\alpha = 0$, $\alpha = 0.4$, $\beta = 1$, and $\Gamma_0 = 0.2$.

Figure 2: $A(\omega)$ versus energy for different temperatures. $\lambda = 0.5$, and $t = 0.2$. Other parameters are the same as fig. 1.

Figure 3: Transmission coefficient as a function of energy. Parameters are the same as fig. 1. $\lambda = 0.5$ in fig. b.

Figure 4: The current versus voltage for $\lambda = 0.5$ (solid line) and $\lambda = 0$ (dashed line) at $kT = 0$ (gray) and $kT = 1$. Inset shows the conductance. Parameters are $\varepsilon_i = 3$, $t = 2\Gamma_0 = 0.4$.

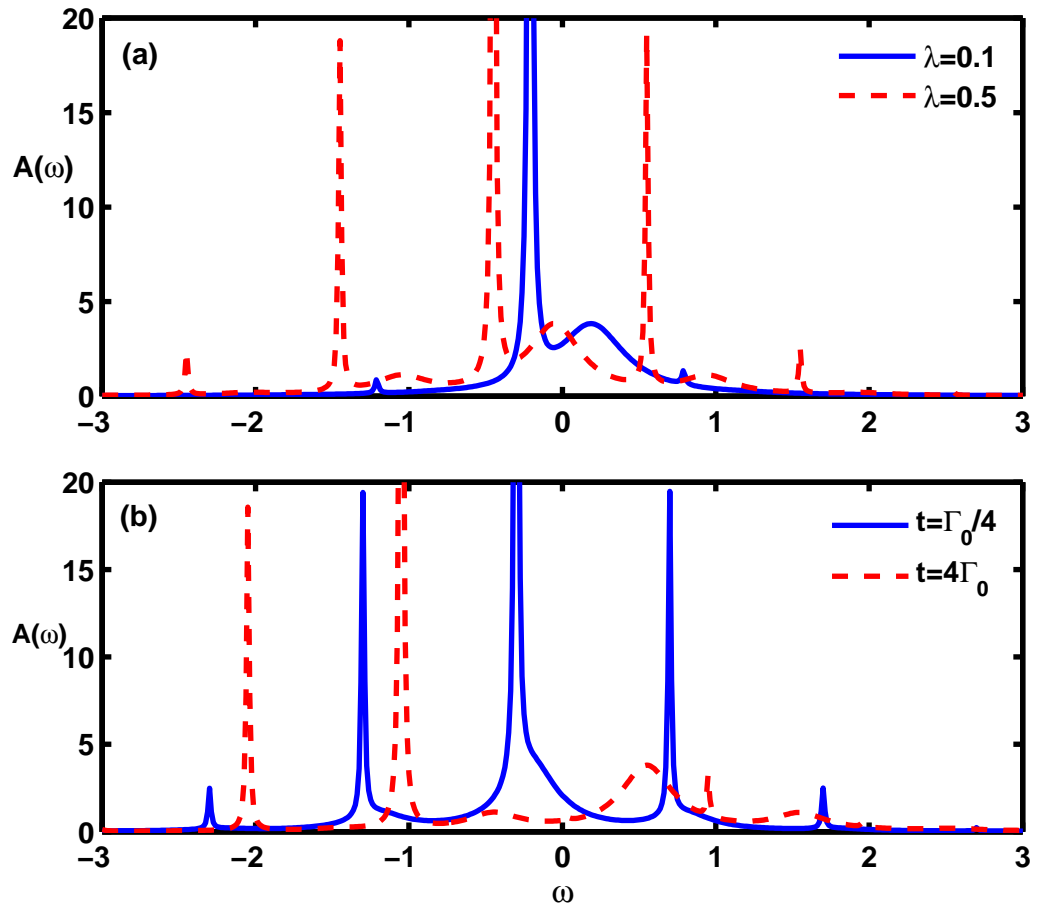


Figure 1:

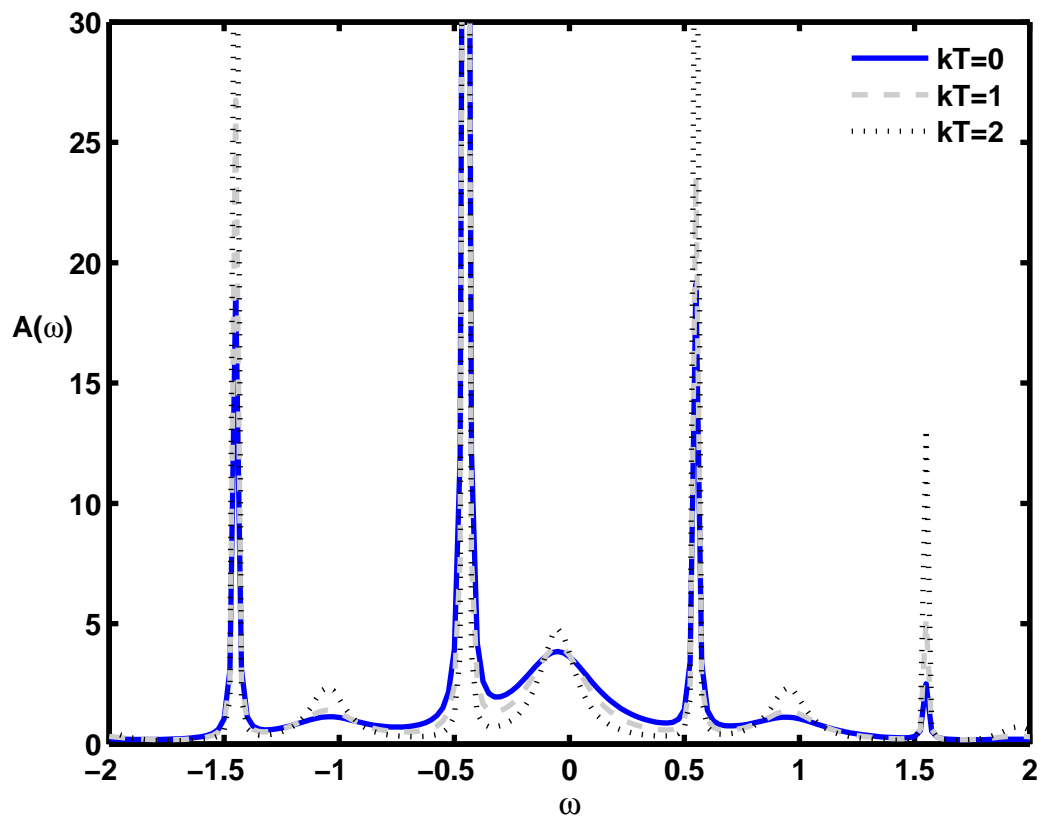


Figure 2:

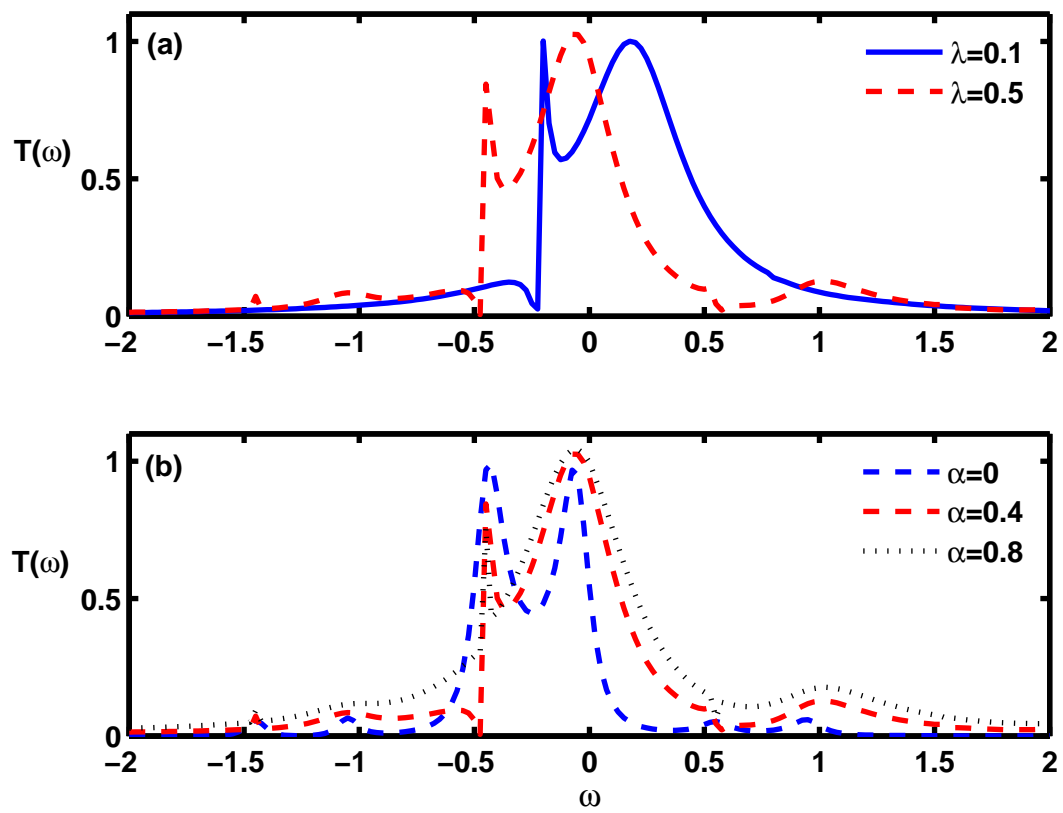


Figure 3:

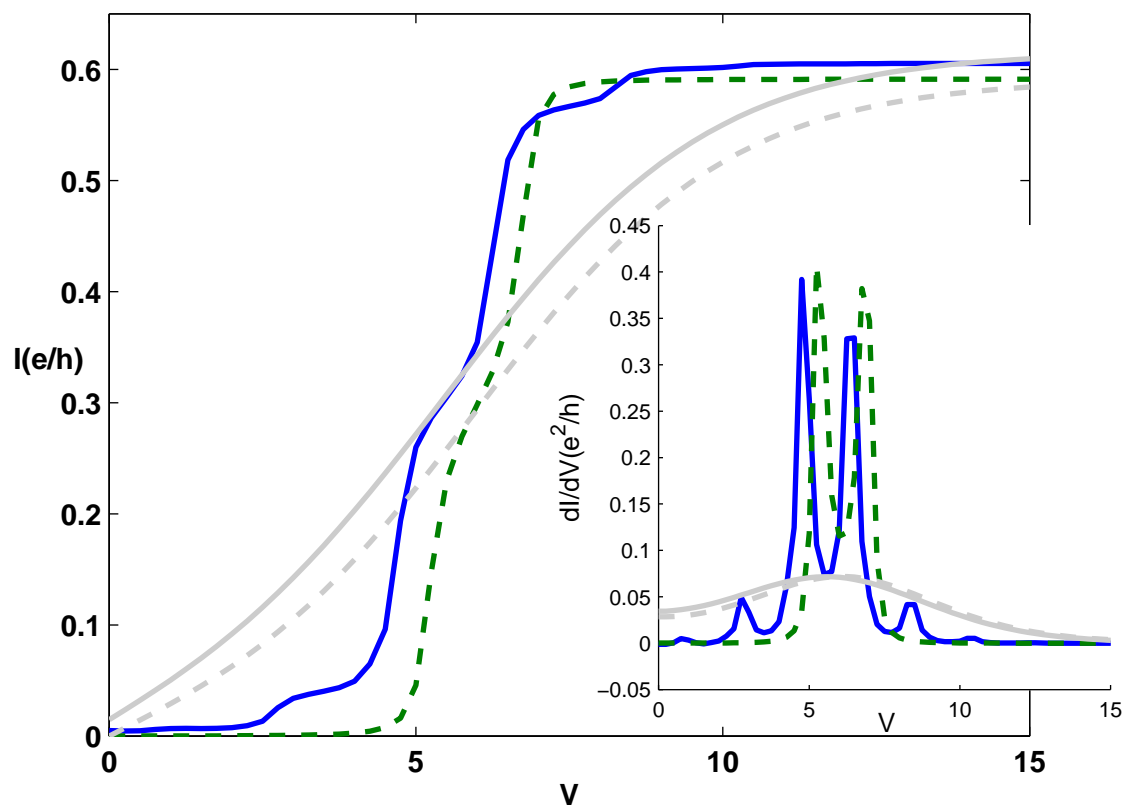


Figure 4: